

Statistical analysis of $^{13}\text{C}(^{13}\text{C},\alpha)^{22}\text{Ne}$

G. P. Gilfoyle and H. T. Fortune

Physics Department, University of Pennsylvania, Philadelphia, Pennsylvania 19104

(Received 13 February 1985)

Complete angular distributions ($\vartheta_{\text{c.m.}} = 9^\circ - 90^\circ$) for the reaction $^{13}\text{C}(^{13}\text{C},\alpha)^{22}\text{Ne}$ in the energy range $E_{\text{c.m.}} = 6.25 - 13.38$ MeV have been subjected to a battery of tests to determine the existence of a significant nonstatistical component in the cross section. The autocorrelation function, distribution of cross sections, and channel correlations were investigated. The data were also compared with the predictions of Hauser-Feshbach calculations. A large nonstatistical component was found in all tests and comparisons.

I. INTRODUCTION

The discovery of resonant structure in the $^{12}\text{C} + ^{12}\text{C}$ system has spawned decades of theoretical and experimental work to reveal the nature of the phenomenon in this system and similar ones.¹⁻⁴ Only a few of these studies, however, have explored the effect of valence particles on the nuclear structure. An understanding of these effects is vital since many current theories predict a smoothing out of resonant behavior when one or two nucleons are added to α -particle nuclei such as ^{12}C or ^{16}O .^{2,4} Some work has been done to discover the influence of one valence neutron in the carbon-carbon system. Investigations of fusion and α decay of $^{12}\text{C} + ^{13}\text{C}$ have shown that system to behave in a manner similar to $^{12}\text{C} + ^{12}\text{C}$.^{5,6} The effect of two valence neutrons has been examined in the carbon-carbon system. Fusion experiments in the $^{13}\text{C} + ^{13}\text{C}$ system found little or no indication of resonant phenomena,²⁻⁹ while elastic scattering and transfer reaction experiments provided evidence of nuclear molecular orbital effects.¹⁰ Reaction studies of $^{12}\text{C} + ^{14}\text{C}$ (which passes through the same intermediate nucleus as $^{13}\text{C} + ^{13}\text{C}$) did not show structure in the α channel beyond what is explainable with the statistical model,^{11,12} but inelastic scattering and transfer reaction data suggest otherwise.¹³ Thus, the evidence for strong resonant behavior in ^{26}Mg is tantalizing, but not definitive. The subject demands clarification. We chose to investigate the $^{13}\text{C}(^{13}\text{C},\alpha)^{22}\text{Ne}$ reaction over a broad energy range and in great depth as a step towards this clarification.

The most difficult and controversial experimental problem in this field is the identification of resonances in the midst of Ericson fluctuations. There exist a number of criteria that can be applied to a data set to aid in such an identification. The first and most obvious is to locate peaks in an excitation function for a given state or combination of states. The technique is most reliable when one examines the angle-integrated cross section to avoid misinterpretations arising from interference effects. Interference between the nonresonant reaction amplitudes that contribute to the cross section can cause rapid fluctuations in the excitation function at selected angles, but these may not indicate any enhancement in the integrated cross section. If fluctuations do exist in the data set, then

more stringent tests must be applied to distinguish true resonances from statistical fluctuations. The average behavior can be examined. The autocorrelation function, which will be described in detail below, is used to set limits on the nonstatistical or direct component of the cross section. In this discussion the term "direct" will refer to any nonstatistical process which contributes to the cross section. The distribution of cross sections about their average can in certain cases be used to establish the existence of a direct component. The shape of the distribution can be quite sensitive to the direct part of the reaction.

The energy dependent behavior of the data set can also be studied for resonant effects. As mentioned above, one can simply look for peaks in the excitation functions, but this is not enough to separate resonances from statistical fluctuations. The most important test is to look for channel correlations in the data. If a true resonance has been made in the intermediate nucleus then one expects the strength in some if not all exit channels to be enhanced. The statistical model of the decay of a compound nucleus can be used to predict the energy-averaged values of certain observables. These can then be compared with the average behavior of the data set. Finally, the energy dependence of the shape of the differential cross section is characteristic of the amplitudes of different l values involved in the reaction. One expects that one or at least just a few amplitudes will dominate the cross section "on resonance" and that it can be decomposed into its constituents. The analysis techniques just described all suffer from ambiguities or imprecisions of varying degrees which have been cataloged in the literature.^{14,15} The result of any single test cannot be taken as unequivocal proof of the existence or nonexistence of a direct component in a reaction. One should use all the tools available, and if all the results point towards a single outcome then one can have confidence in that conclusion.

In this paper we will present data for the $^{13}\text{C}(^{13}\text{C},\alpha)^{22}\text{Ne}$ reaction. The angle-integrated cross sections over a broad energy range for the ground state and the first two excited states will be exhibited along with the results of a variety of tests and comparisons which establish the direct nature of most of the cross section. We have used autocorrelation analysis, examined the distribu-

tion of cross sections, searched for channel correlations, and made comparisons with the predictions of the statistical model. The outcome of each method applied is characteristic of a large direct component.

II. EXPERIMENTAL METHOD AND RESULTS

A ^{13}C beam was extracted from the University of Pennsylvania FN tandem Van de Graaff accelerator and bombarded self-supporting enriched (97%) ^{13}C foils of mean areal density $20\ \mu\text{g}/\text{cm}^2$. The incident beam lost about 60 keV (c.m.) in the target. Alpha particles were detected with two position-sensitive slice detectors designed and built by Zurmühle and Csihas.¹⁶ Thin nickel foils placed in front of each detector stopped particles heavier than α 's. Angular distributions were measured usually in 125 keV (c.m.) steps in the range $E_{\text{c.m.}} = 6.25\text{--}13.38$ MeV. Typically, one detector was kept fixed at back angles (i.e., near $\vartheta_{\text{c.m.}} = 90^\circ$) while the second slice detector was moved to cover all the forward angles. Each distribution spanned the region $\vartheta_{\text{c.m.}} = 9^\circ\text{--}90^\circ$ and contained data at 141 angles. The angular resolution was about 0.6° . Two solid state detectors at $\pm 10^\circ$ were used as beam monitors. Only the first few states in ^{22}Ne were resolvable because at excitation energies greater than 4.65 MeV, impurity peaks from $^{12}\text{C}(^{13}\text{C}, \alpha)^{21}\text{Ne}$ dominated the spectrum. Differential cross sections were extracted for the 0^+ ground, $2^+(1.275\text{ MeV})$, and $4^+(3.357\text{ MeV})$ states at 54 bombarding energies.

III. ANALYSIS

The excitation functions for the angle-integrated cross sections are shown in Figs. 1–3. They exhibit gross structures of width $\Gamma_{\text{c.m.}} \approx 1.0\text{--}2.0$ MeV which are fragmented into narrower structures of width $\Gamma_{\text{c.m.}} \approx 200\text{--}400$ keV. The magnitude of the fluctuations is considerably more pronounced than what would be expected by the statistical model.¹⁷ This observation will be put on a more quantitative basis below. The problem of separating the resonant structure from the “noise” of statistical fluctuations is critical as described above. We calculate the autocorrelation function defined by the relation

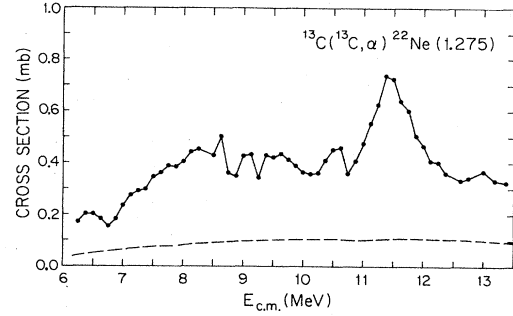


FIG. 2. Same as Fig. 1 for the ^{22}Ne excited 2^+ state at 1.275 MeV.

$$R(\Gamma, \epsilon) = \frac{\langle \sigma(E) \sigma(E + \epsilon) \rangle}{\langle \sigma(E) \rangle \langle \sigma(E + \epsilon) \rangle} - 1, \quad (1)$$

where $\sigma(E)$ is the angle-integrated cross section at energy E , ϵ is the energy interval, and Γ is the average width or coherence width of levels in the compound nucleus. The autocorrelation function can also be described by a Lorentzian shape so that

$$R(\Gamma, \epsilon) = \frac{\Gamma^2}{\Gamma^2 + \epsilon^2} \frac{1 - Y_{D_k}^2}{N_k}, \quad (2)$$

where N_k is the effective number of channels contributing to a particular exit channel k , and Y_{D_k} is the ratio of the average direct cross section to the average total cross section. The mean square deviation, $R(\Gamma, 0)$, for each state can be used to put limits on Y_{D_k} and N_k . At 0° , N_k is one and it rises to a maximum at 90° of $N_k = g/2$ (g even) or $(g+1)/2$ (g odd)—with

$$g = (2i+1)(2I+1)(2i'+1)(2I'+1),$$

where i and I are the spins of the target and projectile and i' and I' are the spins of the final fragments.¹⁸ The $R(\Gamma, 0)$ values and the allowed ranges of Y_{D_k} and N_k obtained in the present work are shown in Table I. For the ground state the smallest allowable Y_{D_k} indicates that fully 89% or more of the cross section is nonstatistical. For the two excited states the case is not as clear. Because of the nonzero spins of these final states the allowed number of channels that can possibly contribute is greatly in-

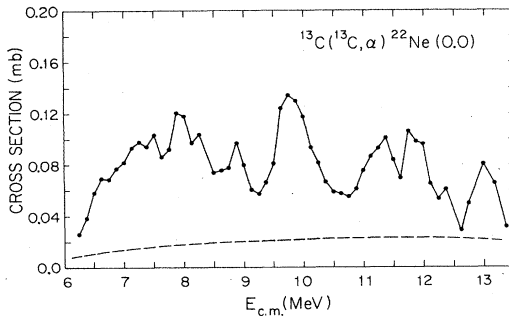


FIG. 1. Excitation function of the angle-integrated cross section for the 0^+ ^{22}Ne ground state. The dashed curve is the energy-averaged statistical-model prediction.

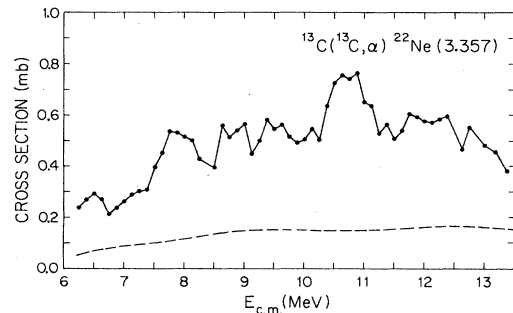


FIG. 3. Same as Fig. 1 for the ^{22}Ne excited 4^+ state at 3.357 MeV.

TABLE I. Autocorrelation results for $^{13}\text{C}(^{13}\text{C},\alpha)^{22}\text{Ne}$.

Channel	$R(\Gamma,0)$	Min	N_k		Min	Y_{D_k}	
			Mean	Max		Mean	Max
0^+	0.101	1	1.5	2	0.89	0.92	0.95
2^+	0.096	1	5.5	10	0.20	0.69	0.95
4^+	0.073	1	7.37	13.73 ^a	0.0	0.68	0.96

^aThe value of N_k for which Y_{D_k} goes to zero.

creased, creating an ambiguity in the analysis. In fact, for the 4^+ state the limit on N_k is not that set by the factor g mentioned above, but by the fact that Y_{D_k} goes to zero for large N_k . Thus, all values of Y_{D_k} are allowed from 0.96 down to zero. The 2^+ level is only a little better with the allowed range of Y_{D_k} going from 0.95 to 0.20. While these results overlap with the limits on Y_{D_k} for the ground state no strong conclusions can be drawn. Finally, we determined the coherence width, Γ , of the transition to the ^{22}Ne ground state to be 125 keV (c.m.) by measuring the width of $R(\Gamma,\epsilon)$ at half its maximum value at $\epsilon=0$.

The uncertainty in measuring $R(\Gamma,0)$ arises mostly from the finite range of the data. The relative standard deviation is defined by

$$\Delta R(\Gamma,0) = \left[\frac{1+R(\Gamma,0)}{n} \right]^{1/2}, \quad (3)$$

where n is the number of data points in the sample. The fractional uncertainty in Y_{D_k} is then

$$\frac{\Delta Y_{D_k}}{Y_{D_k}} = \frac{1}{2} \left[\frac{R(\Gamma,0)}{1-R(\Gamma,0)} \right] \frac{\Delta R(\Gamma,0)}{R(\Gamma,0)}. \quad (4)$$

However, even large uncertainties in the values of $R(\Gamma,0)$ do not greatly change the values of Y_{D_k} . A 30% uncertainty in $R(\Gamma,0)$ for the ground state implies an uncertainty in Y_{D_k} of only 0.2%. It is not expected that an Ericson fluctuation analysis can determine Y_{D_k} with such a high degree of accuracy.^{19,20} A more conservative approach would be to assert that the autocorrelation analysis supports the conclusion that most of the cross section is direct, but cannot distinguish between an 80% component and a 90% one. Our measured values of Y_{D_k} are also consistent within this uncertainty with other techniques which will be discussed below.

The frequency distribution of cross sections for the ground state is shown in Fig. 4. We define $Y_k = \sigma_k(E) / \langle \sigma_k(E) \rangle$ where $\langle \sigma_k(E) \rangle$ is the running average with an interval size $\Delta E_{\text{c.m.}} = 1.50$ MeV. The method used to determine the width of the averaging interval will be discussed below. We expect the probability density of Y_k to be given by^{14,21}

$$p(Y_{D_k}) = \frac{N_k}{Y_{D_k}} \left[\frac{Y_k}{Y_{D_k}} \right]^{N_k-1} \exp \left[-N_k \left[\frac{Y_k + Y_{D_k}}{1 - Y_{D_k}} \right] \right] \times I_{N_k-1} \left[\frac{2N_k(Y_k Y_{D_k})^{1/2}}{1 - Y_{D_k}} \right], \quad (5)$$

where I_N is a modified Bessel function of order N . The solid curve in Fig. 4 represents the probability density calculated with Y_{D_k} and N_k from the autocorrelation analysis results of Table I. The curve is insensitive to the ambiguities in Y_{D_k} and N_k . Different combinations of Y_{D_k} and N_k allowed by Eq. (2) make no visible change in

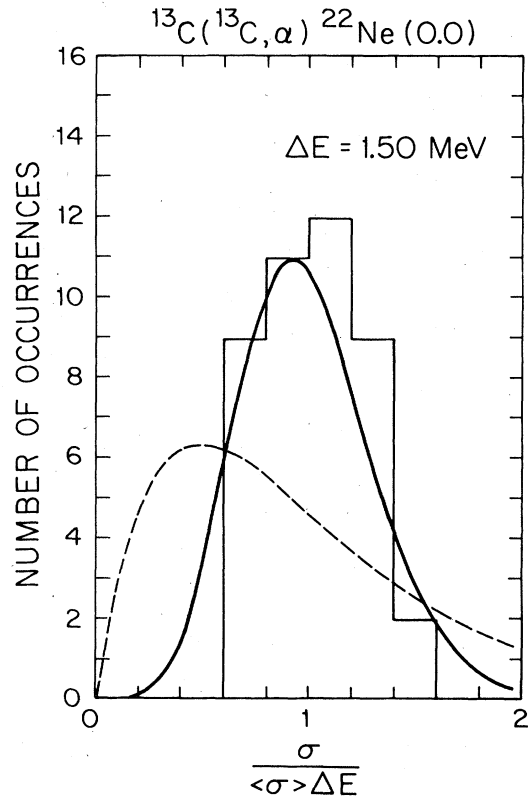


FIG. 4. The distribution of cross sections for the ^{22}Ne ground state. The solid curve is $p(Y_k)$ calculated with the parameters from Table I and the dashed curve is $p(Y_k)$ with $Y_{D_k}=0.0$ and $N_k=2.0$.

TABLE II. Optical-model parameters for Hauser-Feshbach calculations.

Channel	Reference	V_R (MeV)	R_R (fm)	a_R (fm)	V_I (MeV)	R_I (fm)	a_f (fm)
$^{13}\text{C} + ^{13}\text{C}$	7	16.0	6.35	0.45	$0.22E_{\text{c.m.}}$	6.35	0.30
$n + ^{25}\text{Mg}$	26	A^a	5.121	0.660	B^b	4.936	0.580
$\alpha + ^{22}\text{Ne}$	27	204.40	3.78	0.576	73.27	2.36	0.130

$$^a A = 47.01 - 0.267E_{\text{c.m.}} - 0.0018E_{\text{c.m.}}^2.$$

$$^b B = 9.52 - 0.53E_{\text{c.m.}}.$$

the distribution. The probability density agrees quite well with the data. If Y_{D_k} were really zero the closest one could get to the experimental distribution would be to set $N_k = 2.0$. The result would be the dashed curve in Fig. 4. The data are clearly not represented by any such distribution—thus emphasizing the difference between the measured $Y_k(E)$ and the predictions of the statistical model. The probability densities for the 2^+ and 4^+ states predicted by the autocorrelation analysis are consistent with the data within the uncertainty in Y_{D_k} and N_k , but again suffer from the same ambiguities since the distributions are insensitive to changes allowed by Eq. (2). Thus, the distribution of cross sections for the ground state is consistent with the autocorrelation analysis indicating a large nonstatistical component in the angle integrated cross section. The 2^+ and 4^+ distributions are also consistent within uncertainties with the same analysis, but suffer from the previous ambiguities.

Energy-averaged total cross sections were calculated using the Hauser-Feshbach expression in the computer code STATIS.²² The exit channels included in the calculation were the following: $^{13}\text{C} + ^{13}\text{C}$, $\alpha + ^{22}\text{Ne}$, $n + ^{25}\text{Mg}$, $2n + ^{24}\text{Mg}$, $p + ^{25}\text{Na}$, and $t + ^{23}\text{Na}$. Transmission coefficients derived from the optical-model were input for the $^{13}\text{C} + ^{13}\text{C}$, $\alpha + ^{22}\text{Ne}$, and $n + ^{25}\text{Mg}$ channels and the code's internal parametrization was used for the remaining channels which make only a small contribution to the fusion cross section. The input parameters for STATIS and the optical-model parameters used to calculate the transmission coefficients are listed in Tables II and III. The ratio of the average Hauser-Feshbach cross section, $\langle \sigma_{\text{HF}} \rangle$, to the average of the data, $\langle \sigma_{\text{total}} \rangle$, is 0.24 for the ground state and 0.28 for both the 2^+ and 4^+ states. This ratio yields $Y_{D_k} = 0.72$ for the ground state—a value that is consistent with the previous results within the uncertainties discussed above. A value of $Y_{D_k} = 0.72$ for the excited states also agrees with the autocorrelation analysis and distribution of the cross sections. The Hauser-Feshbach calculations further support the notion that the statistical model accounts for only a small fraction of the measured cross section for the first three states.

The existence of correlations between different channels

is usually a distinctive feature that separates resonances from a fluctuating background.^{14,23} Consider the deviation function

$$D(E) = \frac{1}{N} \sum_{k=1}^N \left[\frac{\sigma_k(E)}{\langle \sigma_k(E) \rangle} - 1 \right], \quad (6)$$

$$= \frac{1}{N} \sum_{k=1}^N (Y_k - 1), \quad (7)$$

where N is the number of excitation functions and $\langle \sigma_k(E) \rangle$ is a running average of the angle integrated cross section with an averaging interval of $\Delta E_{\text{c.m.}} = 1.50$ MeV. The size of the interval is determined by the behavior of $D(E)$ as the interval is increased. When it becomes sufficiently greater than the coherence width of levels in the compound nucleus the shape of $D(E)$ will remain essentially constant. The averaging interval we obtained in this manner is consistent with the coherence width of 125 keV that we measured with the autocorrelation function. We use the running average in order to eliminate any kinematic effects on the average cross section, such as the presence of the Coulomb barrier at $E_{\text{c.m.}} \approx 6.4$ MeV. The probability density $p(Y_k)$ for a given channel, Y_k , is given above by Eq. (5). The probability distribution for the deviation function, $p(D)$, is given for statistically independent Y_k by the Fourier transform of the product of the characteristic functions, $\Phi_k(t)$, of the original probability densities for the different states, $p(Y_k)$.²³ The characteristic function for each channel is

$$\Phi_k(t) = \int_0^\infty p_k(Y_k) e^{itY_k} dY_k. \quad (8)$$

The characteristic function of $D(E)$ is then

$$\Phi_D(t) = \prod_{k=1}^N e^{-it/N_k} \Phi_k \left[\frac{t}{N_k} \right]. \quad (9)$$

The probability density of $D(E)$ is given by the Fourier transform of Φ_D ,

$$p(D) = \frac{1}{2\pi} \int_{-\infty}^\infty \Phi_D(t) e^{-iDt} dt. \quad (10)$$

We can now calculate the probability or confidence level

TABLE III. Level density parameters (Ref. 7).

	^{25}Mg	^{22}Ne	^{25}Na	^{24}Mg	^{23}Na	^{13}C
a (MeV $^{-1}$)	3.13	3.52	3.13	2.79	2.88	1.95
Δ (MeV)	-1.40	1.50	-1.20	2.10	-1.00	2.250

for $D(E)$ from Eqs. (5) and (8)–(10) using the parameters from the autocorrelation analysis. The percentage of data points with a deviation greater than x_T or less than x_B is defined by²³

$$Q(x_T) = \int_{x_T}^{\infty} p(D) dD, \quad (11)$$

$$Q(x_B) = \int_{-\infty}^{x_B} p(D) dD. \quad (12)$$

In Fig. 5 we have plotted $D(E)$ for the first three states in ^{22}Ne along with the lines representing the 3% confidence levels. Because we are using a running average the points that are closer to the end of the data set than one-half the averaging interval cannot be treated properly. Those points have not been included. Outside the 3% level we observe four peaks containing nine data points out of a total of forty-six data points (20%). Whereas statistical considerations would lead us to expect at most a few events (one or two), we find nine. Thus, we observe strong evidence for correlated structure in $^{13}\text{C}(^{13}\text{C},\alpha)^{22}\text{Ne}$.

One expects that the ground state transition at these correlated maxima should have angular distributions dominated by a few l values. In Fig. 6 we exhibit the differential cross sections for the ^{22}Ne ground state at the energies corresponding to the strongly correlated peaks in $D(E)$. Based simply on the number of minima in the angular distributions the structures at 8.0 and 11.75 MeV are dominated by $l=4$ and $l=10$, respectively. The grazing l values at these energies are approximately 6 and 9.5. A more sophisticated analysis of the data performed by us and presented in Ref. 24 for the region around the 9.63 MeV peak indicates that several l values contribute about equally at this energy, but the most important amplitudes are those for $l=4$ and $l=6$. The same technique applied at the 11.38 MeV maximum shows it to have sizable contributions from amplitudes for both $l=6$ and $l=10$. The distributions at all the maxima except the 9.63 MeV one are highly oscillatory—clearly suggesting that only a few l values dominate the reaction amplitude at these energies. A more detailed presentation of the partial wave decomposition will be the subject of a future paper.

A wide variety of other statistical tests are presented in the literature.^{14,15} However, these are generally not as effective at sifting out a resonant component of the cross

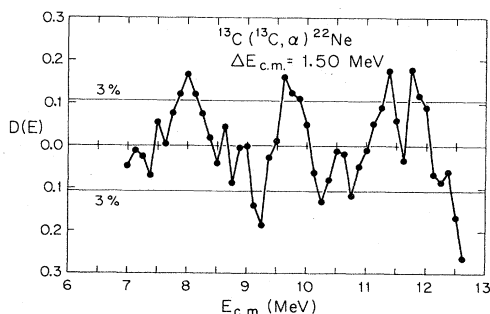


FIG. 5. Deviation function for the first three states in ^{22}Ne . The solid lines represent the 3% confidence levels described in the text.

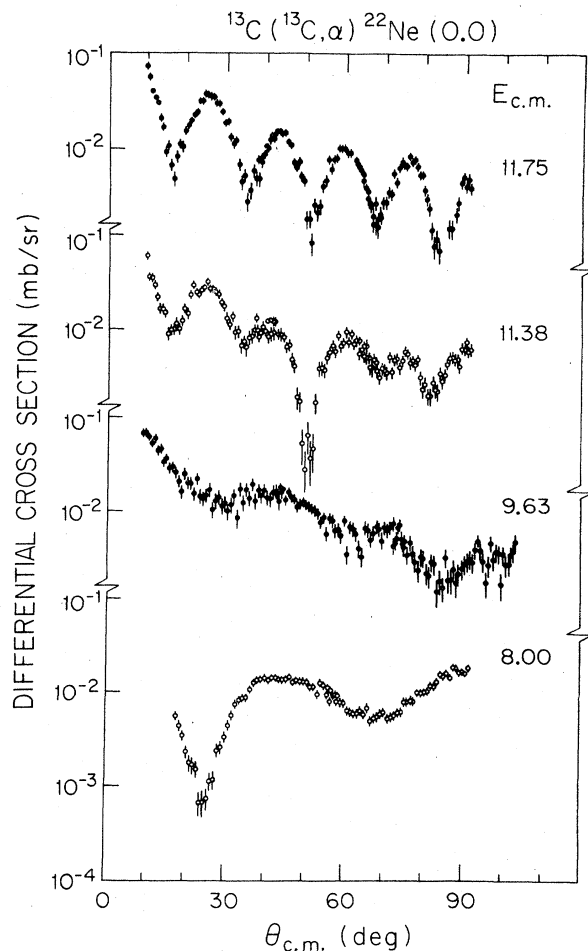


FIG. 6. Ground state angular distributions at $E_{\text{c.m.}} = 8.0, 9.63, 11.38,$ and 11.75 MeV. These correspond to the maxima in $D(E)$.

section from the background in the case of heavy ions.^{14,25} While no method is foolproof, the techniques we have applied are the most reliable.

IV. CONCLUSION

The compelling conclusion of our analysis is that the $^{13}\text{C}(^{13}\text{C},\alpha)^{22}\text{Ne}$ reaction proceeds largely via a nonstatistical mechanism. Despite any ambiguities in a particular test, every one of our results points towards this result. We have found that the average behavior of the angle-integrated cross sections for the ground state and the first two excited states in ^{22}Ne exceed the statistical expectation by a factor of about 4. Just as important, we find strong evidence of correlations between different exit channels in $^{13}\text{C}(^{13}\text{C},\alpha)^{22}\text{Ne}$ at four energies. The angular distributions at these energies are not completely dominated by a single l value, but it is clear that only a few l values are contributing to the cross section for at least three of the correlated maxima. A number of theoretical models like the band-crossing model, the double resonance mechanism, coupled-channel models, and the barrier top

model have had varying degrees of success in describing similar data in other systems.^{3,4,10} Very few calculations, though, exist in the literature for a two valence nucleon case such as $^{13}\text{C}+^{13}\text{C}$. The density of states here is about 10^3 times that of $^{12}\text{C}+^{12}\text{C}$, yet we still observe narrow structures that have not dissolved into a sea of compound

nuclear states. A full understanding of the physical picture of the influence of valence nucleons on heavy-ion resonances remains to be found.

We acknowledge financial support from the National Science Foundation.

-
- ¹T. M. Cormier, *Annu. Rev. Nucl. Part. Sci.* **32**, 271 (1982).
²R. M. Freeman, in *Proceedings of the International Conference on the Resonant Behavior of Heavy Ion Systems, Aegean Sea, 1980*, edited by G. Vorvopoulos (Greek Atomic Energy Commission, Athens, 1981), p. 41.
³R. Koennecke, W. Greiner, Y. Park, and W. Schied, see Ref. 2, p. 163.
⁴W. Greiner, see Ref. 2, p. 391.
⁵D. J. Crozier and J. C. Legg, *Phys. Rev. Lett.* **33**, 782 (1974).
⁶A. D. Frawley, N. R. Fletcher, L. C. Dennis, and K. M. Abdo, *Nucl. Phys.* **A394**, 292 (1982).
⁷J. L. Charvet, R. Dagrass, J. M. Fieni, S. Joly, and J. L. Uzureau, *Nucl. Phys.* **A376**, 292 (1982).
⁸Mohan L. Chatterjee, Lac Potvin, and Bibiana Cujee, *Nucl. Phys.* **A333**, 273 (1980).
⁹B. Heusch, C. Beck, J. P. Coffin, R. M. Freeman, A. Gallman, F. Haas, F. Rami, P. Wagner, and D. E. Alberger, *Phys. Rev. C* **23**, 1527 (1981).
¹⁰S. K. Korotky, K. A. Erb, R. L. Phillips, S. J. Willet, and D. A. Bromley, *Phys. Rev. C* **28**, 1 (1983).
¹¹W. Galster, P. Dück, H. Frölich, W. Treu, and H. Voit, *Nucl. Phys.* **A277**, 126 (1977).
¹²M. Feil, W. von Oertzen, H. G. Bohlen, A. Gamp, and R. L. Walter, *Z. Phys.* **260**, 271 (1973).
¹³R. M. Freeman, F. Haas, and G. Korschinek, *Phys. Lett.* **90B**, 229 (1980).
¹⁴K. A. Eberhard, see Ref. 2, p. 353.
¹⁵L. C. Dennis, S. T. Ahorton, and K. R. Cordell, *Phys. Rev. C* **19**, 777 (1979).
¹⁶R. W. Zurmühle and L. Csihas, *Nucl. Instrum. Methods* **203**, 261 (1982).
¹⁷T. Ericson, *Phys. Rev. Lett.* **5**, 430 (1960).
¹⁸T. Ericson, *Ann. Phys. (N.Y.)* **23**, 390 (1963).
¹⁹K. Jansen and W. Scheid, *Phys. Lett.* **47B**, 431 (1973).
²⁰L. R. Greenwood, R. E. Segel, K. Raghunathan, M. A. Lee, H. T. Fortune, and J. R. Erskin, *Phys. Rev. C* **12**, 156 (1975).
²¹D. M. Brink and R. O. Stephen, *Phys. Lett.* **5**, 77 (1963).
²²R. G. Stokstad, private communication.
²³J. Lang, M. Hugi, R. Müller, J. Sromicki, E. Ungricht, H. Witala, L. Jarczyk, and A. Stralkowski, *Phys. Lett.* **104B**, 369 (1981).
²⁴G. P. Gilfoyle, L. C. Band, R. Gilman, M. Carchidi, K. S. Dhuga, J. W. Sweet, A. H. Wuosmaa, G. S. F. Stephens, R. W. Zurmühle, and H. T. Fortune, *Phys. Rev. C* **32**, 861 (1985).
²⁵P. Braun-Munzinger and J. Barrette, *Phys. Rev. Lett.* **44**, 719 (1980).
²⁶F. Perey and B. Buck, *Nucl. Phys.* **32**, 353 (1962).
²⁷A. A. Cowley, J. C. Van Staden, S. J. Mills, and P. M. Cronje, *Nucl. Phys.* **A301**, 429 (1978).